CHAPTER 2

Compact Wideband Interdigital Bandpass Filter and its Modification Using Spurlines and Defected Ground Structures

2.1 Introduction

As discussed in Chapter 1, Section 1.4, interdigital bandpass filter (IBPF) is well known for its attractive features, such as its compact structure, wide bandwidth and low loss characteristics, but requires the use of grounding microstrip resonators which is usually accomplished with via-holes [Matthaei *et al*. (1964), Hong and Lancaster (2001)]. In conventional IBPF, an unwanted frequency band at around three times the midband frequency is obtained [Hong and Lancaster (2001)], which is not desired for receiver circuitry of a wireless communication system, and hence, it should be suppressed for obtaining wide stopband. For suppressing the unwanted spurious response, a slit configuration in the filter geometry called spurline is devised and reported in the literature [Nguyen and Chang (1985), Tu and Chang (2005), Wang *et al*. (2010), Lingqin *et al*. (2012)]. It offers excellent band gap characteristics but suffers from the limitation of narrow stopband. Various types of defected ground structures (DGSs) are also proposed for obtaining significantly suppressed out-of-band response [Lingqin *et al*. (2012), Shi *et al*. (2012), Chen *et al*. (2009), Ahn *et al*. (2001)]. The available techniques do not fulfil the stringent requirements of a filter for wireless communication applications, such as wide stop- and pass-bands along with compact size and sharp roll-off simultaneously. In the literature [Nie *et al*. (2014), Liang and Chang (2009), Wang *et al*. (2009), Shaman (2012), Chen *et al*. (2013), Tanii and Wada (2014), Chen *et al*.

(2015)], different designs methodologies of BPF are proposed to obtain compact filter size having wide stopband, sharp roll-off and low insertion loss, but simultaneously achieving all the desired characteristics of BPF is difficult.

In this chapter, a compact modified IBPF is described which provide sharp roll-off and wide stopband with reasonably out-of-band unwanted harmonics rejection capability for L-band applications. A combination of two pairs of spurlines and a pair of stepped impedance resonator (SIR)-shaped DGS are introduced in the conventional IBPF which results in the proposed compact filter with the desired response. For the design and optimization of different stages of the proposed filter, Ansys HFSS numerical simulation software was used. The spurious response suppression characteristics of spurlines and DGS are validated using the computed values of corresponding equivalent circuit parameters (*R*, *L*, and *C*). Details about different stages of the filter design using a pair/pairs of spurlines and a pair of SIR-shaped DGS are discussed and all the required simulation and measurement results are presented and compared in this chapter.

2.2 Design and Study of Conventional Interdigital Bandpass Filter (IBPF)

2.2.1 Design of Conventional IBPF

The IBPF consists of five microstrip transmission line resonators, each of which is quarter-wavelength long at the midband frequency of 1.5 GHz. Each line is short-circuited at one end and open-circuited at the other end having alternate orientations. The fringing fields between adjacent resonators are responsible for coupling of microwave energy from input of the filter to its output. The IBPF is compact and requires the use of grounding microstrip resonators, which is usually accomplished with via-holes. The IBPF produces a transmission zero near twice of the midband frequency

and first spurious response is generally observed at around three times the centre frequency of the filter passband [Hong and Lancaster (2001)]. The equations developed for the design of IBPF with coupled line input/output (I/O) can be found in [Matthaei (1962), Dening (1989)].

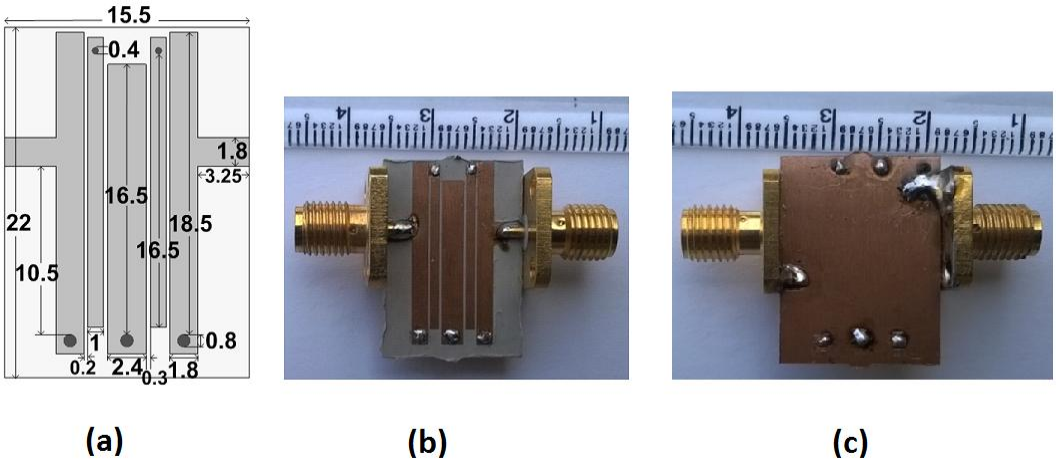

Figure 2.1: (a) Layout of the conventional IBPF with dimensional details (all dimensions are in millimeter). Fabricated prototype of the conventional IBPF (b) top view, and (c) bottom view.

The conventional microstrip IBPF is designed using fifth order Chebyshev lowpass prototype with a passband ripple of 0.1 dB. Figure 2.1(a) shows the layout of conventional IBPF with optimized dimensions. The dimensions of the conventional IBPF are optimized to achieve L-band passband frequency range 1 – 2 GHz with low insertion loss. After optimizing the dimensions of filter geometry to provide desired passband and wide stopband characteristics, the prototype of the conventional IBPF was fabricated with the help of LPKF ProtoMat S103 printed circuit board (PCB) prototyping machine. Top and bottom views of the fabricated prototype of the conventional IBPF are shown in Figures 2.1(b) and 2.1(c). The dielectric substrate, RT/duroid 6010, having dielectric constant of 10.2 and thickness of 1.27 mm was used in the design and fabrication of the prototype of the filter. The variations of filter

parameters: *S*-parameters, group delay and phase response with frequency were simulated using Ansys HFSS software and measured with the help of Keysight E5071C ENA Series Network Analyzer.

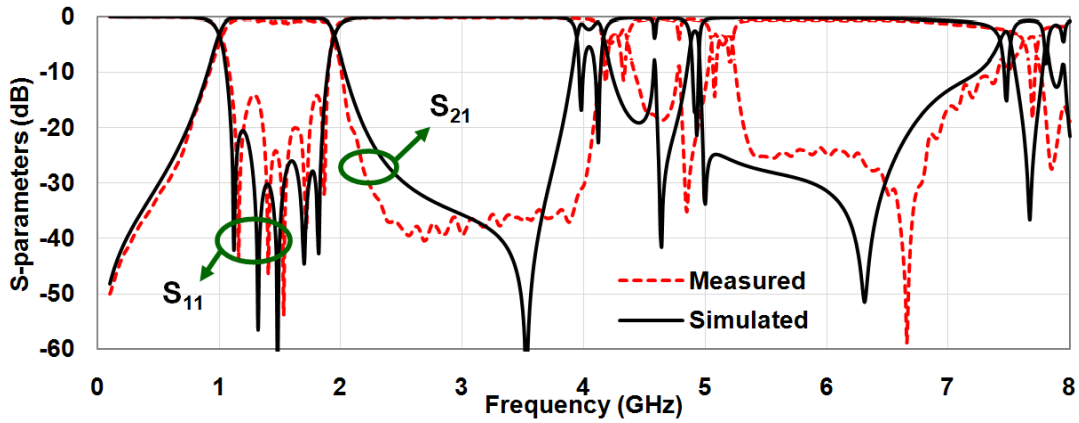

Figure 2.2: Simulated and measured performances of *S*-parameters of the conventional IBPF with frequency.

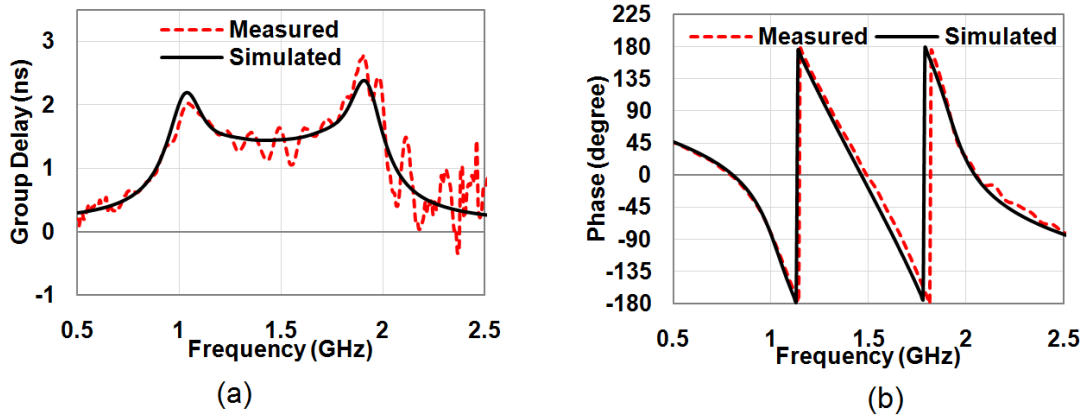

Figure 2.3: Simulated and measured performances of the conventional IBPF with frequency for desired operating band (a) group delay, and (b) phase response.

2.2.2 Results and Discussion

The simulated and measured variations of *S*-parameters of conventional IBPF with frequency are shown in Figure 2.2. The simulated and measured 3-dB fractional bandwidths of the filter are found to be 64% over the frequency range 1.0 – 1.95 GHz and 63% over the frequency range 1.01 – 1.94 GHz respectively. The simulated and

measured values of insertion loss of the conventional filter at centre frequency of passband (= 1.475 GHz) are found to be 0.24 dB and 0.61 dB respectively.

Figure 2.3 shows the variations of simulated as well as measured group delay and phase response of the conventional IBPF with frequency. The group delay response of the filter shows the parabolic behaviour. A constant group delay and linear phase response are required for modern wireless communication systems in order to avoid signal distortion. From Figure 2.3(a), it is observed that in the passband, simulated and measured values of group delay vary over the ranges 1.4 – 2.4 ns and 1.1 – 2.7 ns respectively, which points to near agreement between simulation and measured results. It is observed from Figure 2.3(b) that in the desired passband, almost linear phase response is obtained both through simulation and experimentally, which shows good agreement between the simulation and measured results.

From Figure 2.2, it is also observed that peaks of unwanted harmonics are obtained at frequencies of 4.05, 4.92, 7.47 and 7.78 GHz. For avoiding the interference of signals from L-band system with other frequency bands used for wireless communication, the unwanted harmonic responses should be suppressed. Hence, conventional IBPF structure was modified subsequently for obtaining wide stopband along with miniaturized in size and low insertion loss.

2.3 Design and Investigation of the Proposed Modified IBPF

The conventional IBPF is modified in order to suppress unwanted harmonics and obtain desired performance in passband for the proposed compact BPF. A combination of two pairs of spurlines and a pair of SIR-shaped DGS are introduced in the conventional IBPF which results in the proposed compact filter having the desired responses.

2.3.1 Spurline – Theory and Equivalent Circuit

A spurline is an etched pattern in the form of an L-shaped slit embedded in microstrip line. It can be applied in the design of filter because it has excellent bandgap characteristics [Tu and Chang (2005)]. The layout of spurline is shown in Figure 2.4(a). The slit gap 'g' is responsible for capacitive effect, and narrow line provides inductive effect near the frequencies of interest, where spurious responses are to be suppressed. Significant portion of microwave energy will be trapped around the spurline at or near the frequency to be suppressed due to structure's resonance occurring at the frequency of interest. At resonant frequency, maximum voltage will be dropped across the parallel resonant circuit representing the spurline. This will allow minimum voltage to appear at the output of the circuit. Therefore, unwanted harmonics at or near the resonant frequency of the spurline will be suppressed.

The equivalent circuit of the spurline can be modeled as a parallel *RLC* circuit [Liu *et al*. (2007)], as shown in Figure 2.4(b). The resistor of the spurline equivalent circuit model represents the transmission loss and the radiation effect. The circuit parameters can be extracted based on the transmission line theory and the spectral domain approach [Liu *et al*. (2007)] using the following equations

$$R_i = 2Z_0 \left(\frac{1}{|S_{21,i}|} - 1 \right)_{f=f_i} \tag{2.1}$$

$$C_i = \frac{\sqrt{0.5\left(R_i + 2Z_0\right)^2 - 4Z_0^2}}{2.83\pi Z_0 R_i \Delta f_i} \tag{2.2}$$

$$L_i = \frac{1}{4\left(\pi f_i\right)^2 C_i} \qquad i = 1, 2 \tag{2.3}$$

where Z_0 (= 50 Ω) is the characteristic impedance of the transmission line, f_i is the resonant frequency, $S_{21,i}$ is the insertion loss, and Δf_i is the 3 dB bandwidth of $S_{21,i}$ at f_i.

Due to the introduction of spurlines, spurious responses observed near centre frequencies of 4.05 GHz (f_1) and 7.47 GHz (f_2) are suppressed and corresponding values of equivalent circuit parameters R_1, L_1, and C_1; and R_2, L_2, and C_2 determined on the basis of simulation results shown in Figures 2.5 and 2.6, and Equations (2.1) – (2.3) are 9.9 kΩ, 0.202 nH, and 7.65 pF; and 3.23 kΩ, 0.0277 nH, and 16.4 pF respectively.

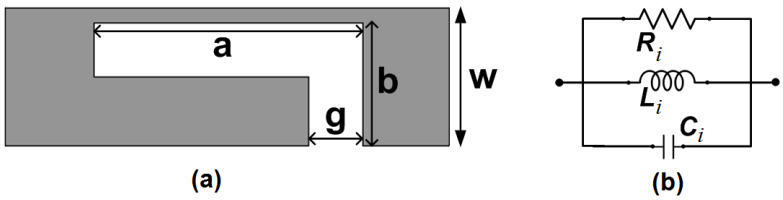

Figure 2.4: (a) Layout of spurline with slit gap 'g', slit height 'b', and slit length 'a', and (b) equivalent circuit model of spurline.

2.3.2 IBPF with One Pair of Spurlines

Figure 2.5(a) shows the IBPF embedded with single pair of spurlines of optimized dimensions for suppression of spurious responses of conventional IBPF to obtain the wide stopband with desired passband performance. The corresponding simulated variations of *S*-parameters versus frequency are given in Figure 2.5(b). It can be observed from Figure 2.5(b) that this IBPF configuration has simulated 3-dB fractional bandwidth of 66 % over the frequency range 0.98 – 1.95 GHz and provides wider stopband as compared with the conventional IBPF. By using a pair of spurlines on first and last resonators, spurious responses observed near centre frequencies of 4.05 GHz and 7.47 GHz in the conventional IBPF are suppressed significantly. But in this configuration, spurious responses are observed near centre frequencies of 4.86 GHz and 7.87 GHz. Therefore, need is felt for further modification in the filter configuration to improve its performance.

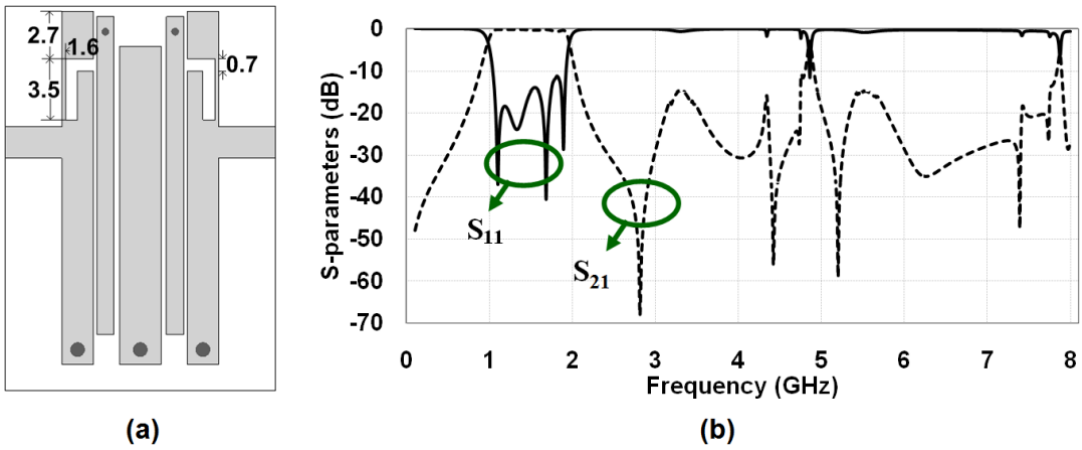

Figure 2.5: (a) Layout of IBPF with single pair of spurlines (all dimensions are in millimeter). (b) Simulated variations of *S*-parameters of IBPF having single pair of spurlines with frequency.

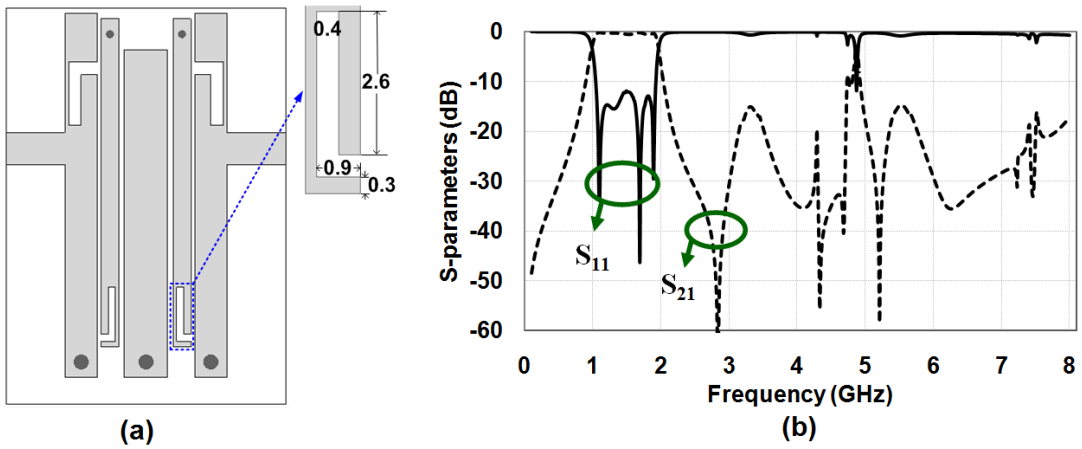

Figure 2.6: (a) Layout of IBPF with two pairs of spurlines (all dimensions are in millimeter). (b) Simulated variations of *S*-parameters of IBPF with two pairs of spurlines with frequency.

2.3.3 IBPF with Two Pairs of Spurlines

Figure 2.6(a) shows the IBPF embedded with two pairs of spurlines of optimized dimensions for further suppression of spurious responses. Figure 2.6(b) reveals the effectiveness of appending two pairs of spurlines in the filter geometry. It can be observed from Figure 2.6(b) that simulated 3-dB fractional bandwidth of this filter configuration is 66% in the frequency range 0.99 – 1.96 GHz. The spurious response is

now observed near the centre frequency of 4.87 GHz only. For the IBPF with two pairs of spurlines, stopband attenuation is better than 15 dB everywhere except near the centre frequency of 4.87 GHz. It can be observed from Figure 2.6 that spurlines on second and fourth resonators are responsible for suppression of unwanted response near the centre frequency of 7.87 GHz. For obtaining miniaturized version of the proposed filter having wider stopband with high suppression, low insertion loss, and sharp roll-off, it is necessary to further modify the design of the filter shown in Figure 2.6(a).

2.3.4 Stepped Impedance Resonator (SIR)-shaped Defected Ground Structure (DGS) – Theory and Equivalent Circuit

A DGS disturbs the current distribution on the surface of ground plane which changes the characteristics of transmission line including its capacitance and inductance. The proposed SIR-shaped DGS consists of wide and narrow etched areas on the metallic ground plane (shown in Figure 2.8) due to which effective capacitance and inductance of the structure will increase. The proposed DGS can be modelled as parallel *LC* resonant circuit and the parameter values can be extracted on the basis of circuit theory. Due to higher impedance offered by the DGS near its resonant frequency, the output voltage of the filter circuit relative to the ground will decrease. Due to the reduction of filter output voltage in the presence of DGS, the suppression of unwanted frequency band, which includes the resonant frequency of DGS, will take place.

The parallel resonant circuit of DGS shown in Figure 2.7(b) forms a part of the BPF circuit. The proposed DGS section provides cut-off frequency and attenuation pole in the frequency range of interest. The attenuation characteristic of the BPF (shown in Figure 2.7(a)) can be explained as the combination of attenuation characteristics of the highpass and lowpass filters having proper cut-off frequencies. The 3-dB cut-off frequency of highpass filter should be lower as compared with that of lowpass filter

(LPF). Hence the attenuation characteristic of the BPF on higher frequency side can be explained through the attenuation characteristic of the LPF. The attenuation pole of the LPF corresponds to the frequency to be suppressed. For the suppression of a frequency band, the equivalent reactance of the filter should be equal to the effective reactance of DGS section. The parameters: capacitance (C) and inductance (L) of the equivalent circuit [shown in Figure 2.7(b)] can be extracted with the help of circuit theory and the simulation results (shown in Figure 2.9) [Ahn *et al*. (2001)].

$$C = \frac{\omega_c}{Z_o g_1} . \frac{1}{\omega_o^2 - \omega_c^2} \tag{2.4}$$

$$L = \frac{1}{4\pi^2 f_o^2 . C} \tag{2.5}$$

where ω_c is the 3-dB higher cut-off frequency of the BPF, Z_o is impedance of the in/out terminated ports, g_1 is the lowpass prototype value representing the inductance, and ω_o is the resonant angular frequency of the parallel LC resonator. For ω_c = 2.05 GHz, ω_o = 4.87 GHz, Z_o = 50 Ω, the values of C and L are found to the 0.2917 pF and 3.6647 nH respectively.

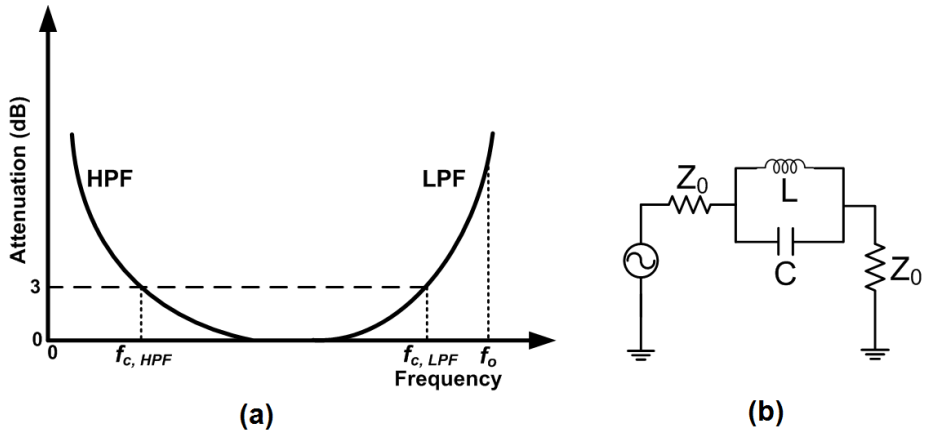

Figure 2.7: (a) Attenuation versus frequency characteristic of the BPF. (b) Equivalent circuit of the proposed DGS.

2.3.5 The Proposed BPF (IBPF with Spurlines and SIR-shaped DGSs)

2.3.5.1 Geometry of the Proposed BPF

Figure 2.8(a) shows the layout of the proposed BPF of optimized dimensions having a combination of two pairs of spurlines and a pair of SIR-shaped DGS which is more compact and provides better response as compared with the BPF configuration shown in Figure 2.6(a). After optimizing the dimensions of filter geometry to provide desired passband and wide stopband, the prototype of the proposed filter was fabricated. The dielectric substrate, RT/duroid 6010, having dielectric constant of 10.2 and thickness of 1.27 mm was used for design and fabrication of the proposed filter. Figures 2.8(b) and 2.8(c) show top and bottom views of the fabricated prototype of the proposed BPF. The variations of filter parameters: *S*-parameters, group delay and phase response with frequency were simulated using Ansys HFSS numerical simulation software and measured with the help of Keysight E5071C ENA Series Network Analyzer.

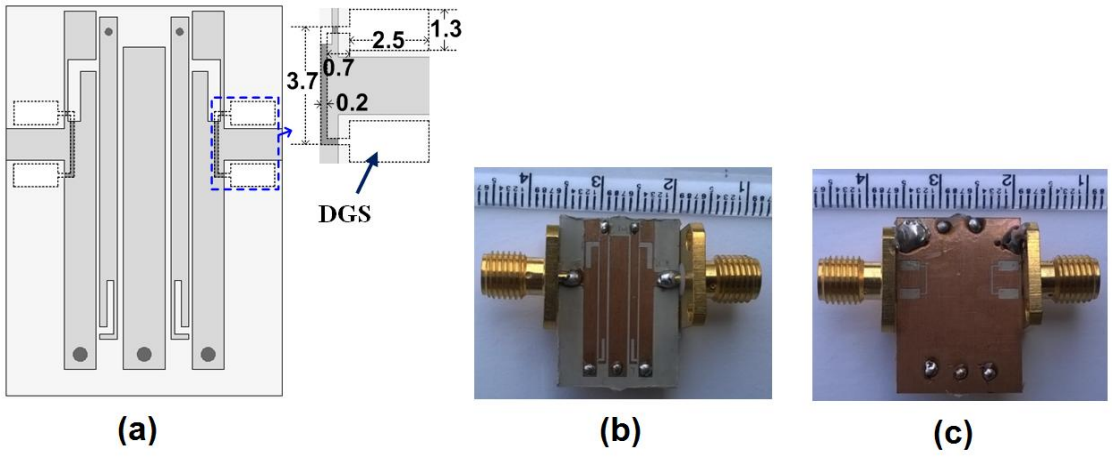

Figure 2.8: (a) Layout of the proposed BPF with two pairs of spurlines and a pair of SIR-shaped DGS (all dimensions are in millimeter). Fabricated prototype of the proposed filter (b) top view, and (c) bottom view.

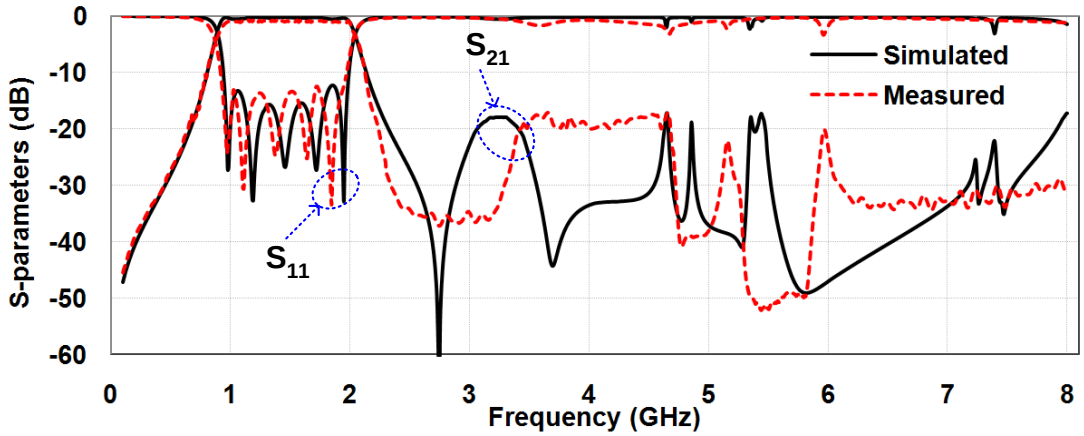

Figure 2.9: Simulated and measured variations of *S*-parameters of the proposed filter with frequency.

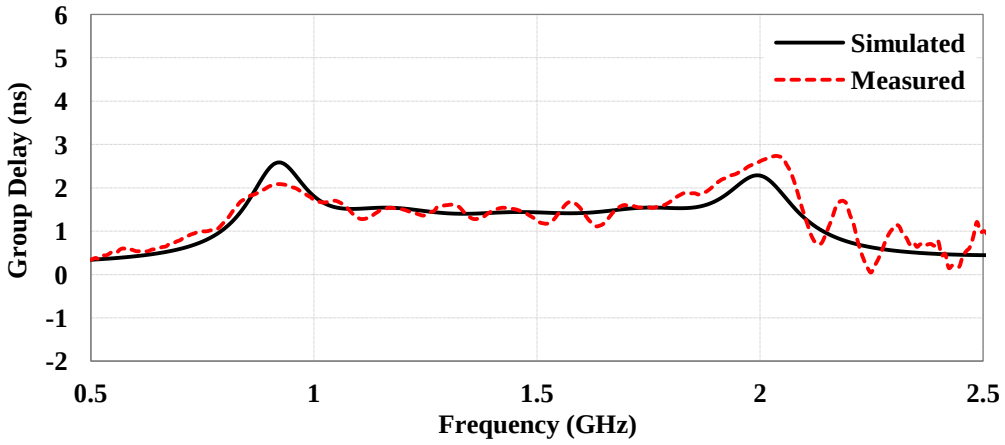

(a)

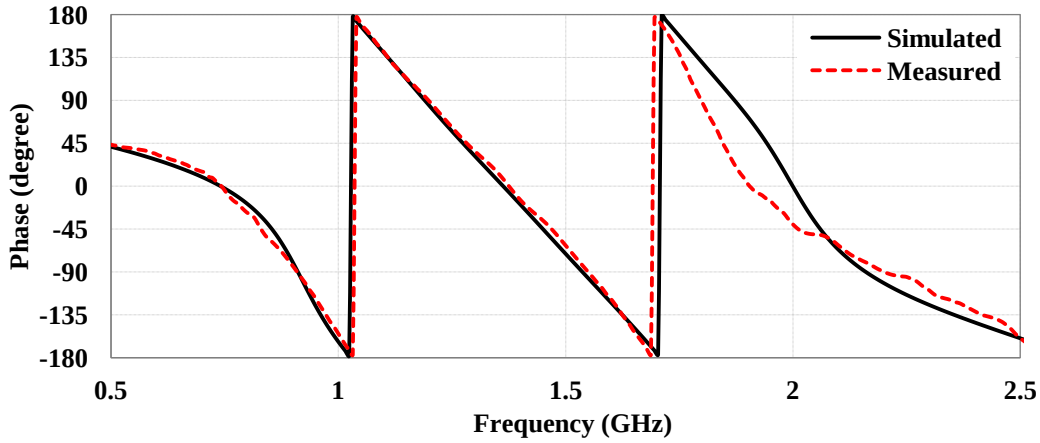

(b)

Figure 2.10: (a) Simulated and measured variations of group delay of the proposed filter with frequency for desired operating band, and (b) simulated and measured variations of phase plot of the proposed filter with frequency for desired operating band.

2.3.5.2 Results and Discussion

The variations of simulated and measured *S*-parameters of the proposed filter with frequency are shown in Figure 2.9. We can observe from Figure 2.9 that due to the introduction of a pair of SIR-shaped DGS, the spurious response observed near 4.87 GHz is suppressed significantly due to effective bandgap characteristic of DGS. The simulated 3-dB fractional bandwidth of the proposed filter is 80% in the frequency range 0.89 – 2.05 GHz. The lower cut-off frequency of the proposed filter is 0.89 GHz, which is 0.11 GHz lower than 1.0 GHz cut-off frequency obtained for conventional IBPF [shown in Figure 2.1(a)]. This result points to the miniaturization of the proposed filter due to the introduction of SIR-shaped DGS. The first transmission zero near higher frequency side of passband occurring at 2.74 GHz with $|S_{21}|$ value of -68 dB reveals sharp roll-off of the proposed filter. The roll-off (RO) rate ζ is defined as [Mirzaee and Virdee (2013)]

$$\zeta = \frac{\alpha_{\max} - \alpha_{\min}}{f_s - f_c} \quad \text{dB/GHz} \tag{2.6}$$

where $\alpha_{\max}$ is the 20 dB attenuation point and $\alpha_{\min}$ is the 3 dB attenuation point; f_s is the 20 dB stopband frequency and f_c is the 3 dB cutoff frequency. The roll-off rates in the lower and upper transition bands for the proposed filter are respectively equal to 75.9 and 60.7 dB/GHz.

All the undesired frequency responses up to 8.0 GHz have been suppressed for obtaining wide stopband with stopband attenuation better than 17 dB. It can be observed from Figure 2.9 that measured 3-dB fractional bandwidth of the fabricated filter is ≈ 79 % in the frequency range 0.87 – 2.01 GHz and the filter provides stopband attenuation better than 16.5 dB. The simulated and measured values of insertion loss $|S_{21}|$ of the proposed filter at centre frequency of passband are 0.35 dB and 0.60 dB, respectively.

From Figure 2.9, it is observed that the simulated and measured results are nearly in agreement with each other excepting minor variations over the frequency range of interest due to fabrication tolerances and measurement errors.

Figure 2.10(a) and (b) show respectively the variations of simulated as well as measured group delay and phase response of the proposed filter versus frequency. From Figure 2.10(a), it is observed that in the desired frequency range of 0.89 – 2.05 GHz, simulated and measured values of group delay vary over the ranges 1.4 – 2.6 ns and 1.1 – 2.7 ns respectively, which points to near agreement between simulated and measured results. It is observed from Figure 2.10(b) that in the desired passband, almost linear phase response is obtained both through simulation and experimentally. The simulation and measured results are nearly in agreement with each other. The deviation in the results may be due to finite SMA connector losses as well as fabrication and measurement errors.

Table 2.1 Performance comparison of the proposed filter with those reported in the literature.

Reference	**FBW (%)**	**IL (dB)**	**Stopband**	**Size ($\lambda_g \times \lambda_g$)**	**ε_r**
[Wang *et al*. (2009)]	60	0.8	3 f_0	0.98 × 0.389	2.56
[Shaman (2012)]	66	≤ 1.0	2.7 f_0	0.775 × 0.24	10.8
[Chen *et al*. (2013)]	36.1	0.4	1.6 f_0	0.39 × 0.40	2.2
[Tanii and Wada (2014)]	44	0.85	2.15 f_0	0.479 × 0.319	10.2
[Chen *et al*. (2015)]	50	0.67	2.5 f_0	0.498 × 0.232	2.65
Proposed filter	**80**	**≤ 0.35**	**6 f_0**	**0.34 × 0.24**	**10.2**

Performance comparison of the proposed filter in respect of the fractional bandwidth (FBW), insertion loss (IL), stopband response, dielectric constant of material used (ε_r) and filter size with those reported in the literature [Wang *et al*. (2009), Shaman (2012), Chen *et al*. (2013), Tanii and Wada (2014), Chen *et al*. (2015)] is given in Table 2.1.

From Table 2.1, it is clear that proposed filter is more compact, has lower insertion loss and wider stop- and pass-bands as compared with the filters reported in the literature.

2.4 Conclusion

The modified miniaturized L-band IBPF with two pairs of spurlines and a pair of SIR-shaped DGS providing sharp roll-off and wide stopband with reasonably suppressed out-of-band harmonics rejection capability has been investigated in this chapter. Starting from conventional IBPF and incorporating two subsequent design modifications, final optimized design of the filter results in its miniaturization and wide stopband characteristic. The equivalent circuits of the spurlines and DGS have been presented and corresponding values of circuit parameters determined. In the proposed filter, a combination of spurlines and DGS has been used for miniaturization and suppression of spurious responses with stopband attenuation better than 17 dB. The highest stopband frequency of the proposed filter is approximately six times the centre frequency of the desired passband. The compactness of the filter along with its wide pass- and stop-bands, sharp roll-off and low insertion loss makes it suitable for L-band wireless communication applications, such as satellite communication, global positioning system, aircraft surveillance system as well as radar and navigation applications.

Further, in order to achieve compact integrated system (combination of filter and antenna) with improved performance for use in the front-end of wireless communication circuitry, the proposed compact L-band BPF having wide stopband, low insertion loss in the passband, sharp roll-off and high out-of-band rejection capability can be integrated with the antenna.

Hence, in the next chapter a compact L-band filtering antenna having sharp cut-off performance and highly suppressed unwanted harmonics is presented.